Chemical Engineering Science, Vol. 40, No. 8, pp. 1379–1385, 1985.
Printed in Great Britain.

0009–2509/85 $3.00 + 0.00
Pergamon Press Ltd.

A PHYSICAL MODEL FOR PREDICTING THE MINIMUM STABLE SLUG LENGTH

ABRAHAM E. DUKLER
Chemical Engineering Department, University of Houston, Houston, TX 77004, U.S.A.

and

DAVID MOALEM MARON and NEIMA BRAUNER†
Department of Fluid Mechanics and Heat Transfer, Faculty of Engineering, Tel-Aviv University, Tel-Aviv, Israel

(*Received* 16 *January* 1984; *in final form* 18 *June* 1984; *accepted* 15 *August* 1984)

Abstract—A physical model for the prediction of the minimum stable slug length in vertical and horizontal slug flows is presented. The model is based on a new concept of recurrent relaxation of the wall boundary-layer at the slug front and its redevelopment at the slug back. Due to the overlapping process in the developing region the probable average stable slug lengths should range between the predicted minimum stable slug length and twice this value. Comparisons with experimental data is satisfactory.

The prediction of the slug length provides an improved method to effect closure for previously existing models for this flow pattern.

INTRODUCTION

The slug flow pattern occurs over a wide range of gas and liquid flow rates. It is commonly encountered during two phase flow in horizontal and vertical pipes. As a result there have been a number of experimental and analytical studies of this flow pattern.

Gas–liquid slug flow in horizontal and nearly horizontal tubes was studied by Dukler and Hubbard [1], including experimental measurements and physical modelling. A further modification was subsequently reported by Nicholson *et al.* [2]. These models can predict the detailed structure of slug flow for given flow rates, fluid properties, tube geometry, measured (or predicted values [3]) of slug frequency and holdup in the liquid slug. Recently, Maron *et al.* [4] proposed a model which evaluates the slug length and the liquid slug hold-up for a given slug frequency. Essentially, the model is based on a concept of periodic distortion of the wall boundary-layers at the front of the slug, followed by a recovery process at the back. Aerated slugs and pure liquid slugs have both been considered. For aerated slugs the model assumes separation of the gas bubbles at the rear of the slug due to buoyancy.

A model for vertical slug flow was recently constructed by Dukler *et al.* [5]. A series of equations were developed based on the physical processes thought to take place during this complex flow pattern. The model permits the prediction of many details of the flow, including the ratio of the liquid slug to the Taylor bubble length. However, a complete closure requires prescription of the slug frequency or the slug length. Dukler *et al.* [5] used the criteria suggested earlier by Taitel *et al.* [9] for this specification.

Experimental observations for water–air systems in vertical upward and horizontal slug flows suggest that the stable slug length, l_s, is relatively insensitive to the gas and liquid flow rates and is fairly constant for a given tube size. The stable slug length has been observed to be of about 12–30D for horizontal slugs (Nicholson *et al.* [2], Hubbard and Dukler [1, 6]). The minimum stable slug length for upward flow in vertical tubes has been observed to be of about 8–16D (Moissis and Griffith [7], Moissis [8]).

Taitel *et al.* [9] suggested that the minimum stable slug length is related to the distance needed to reestablish the normal turbulent velocity distribution in the liquid slug after it is disturbed by the falling liquid film entering at its front. The mixing process between the film and slug was simulated by a wall jet entering a large reservoir. The jet velocity at the pipe centerline was estimated to decay to 5% over a distance of 16D which specified the slug length. Applying this concept to horizontal slugs (Barnea and Brauner [10]) results in a minimum stable slug length of 32D. However, this approach overlooks the viscous effects due to the solid wall, which play a role in determining the developing distance in any entry region phenomena. The purpose of the present study is to incorporate the concepts of periodic relaxation and recovery of the wall boundary layer [4, 11] within a slug unit for determining the stable slug length.

THE PHYSICAL MODEL

The physical concepts developed below are in principle general for horizontal and vertical slug flows. However, for clarity, the presentation proceeds with reference to upward slug flow and then is extended for horizontal configuration.

Upward slug flow

A schematic description of the physical concepts associated in upward slug flow is given in Fig. 1a, b.

†Present address: The Institute of Technical Education, Holon, Israel.

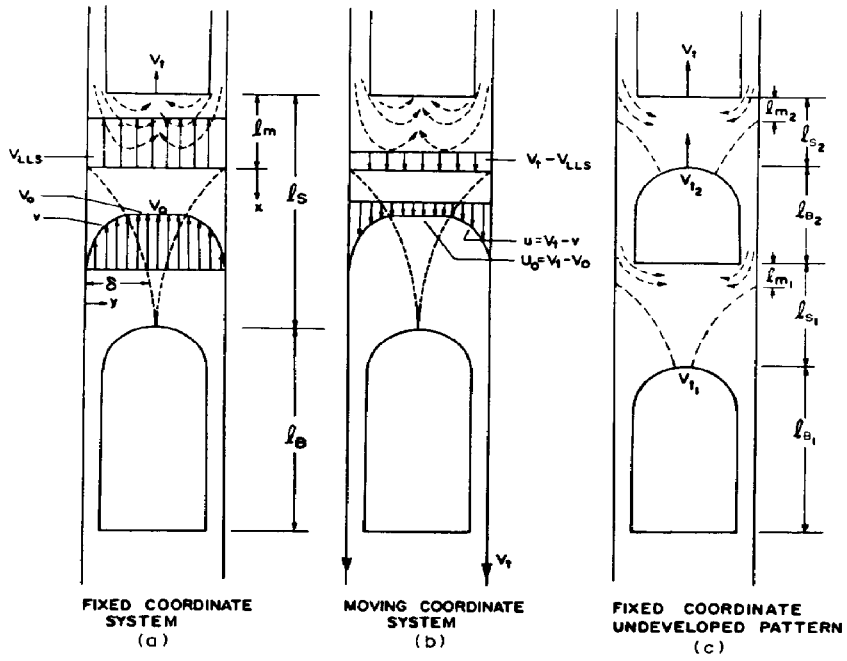

Fig. 1. Schematic description of vertical upward slug flow.

Under the conditions of fully developed flow, successive Taylor bubbles and liquid slugs rise steadily. An idealized axisymmetric flow is considered. The Taylor bubble almost bridges the conduit, leaving a thin counter-current falling film. The falling film merges into the liquid slug, which travels upward overtaking the thin film. Thus, the fluid in the liquid film is continuously picked up by the fast moving slug and is accelerated to the fluid velocity in the liquid slug, forming a mixing eddy which penetrates a distance l_m into the slug front. Simultaneously with this pick-up process the slug sheds liquid from its back, around the nose of the next Taylor bubble thus forming the next falling film. Clearly, when the rate of liquid pick-up at the front equals the rate of liquid shed at the rear the length of the slug stabilizes.

The concept of a mixing vortex at the front, accompanied by a shedding process at the back, implies a recurrent development of the momentum boundary layer in the slug. The boundary layer adjacent to the wall is periodically destroyed (or distorted) in the mixing region at the front of the slug and is reestablished (or recovered) in the body of the slug behind the mixing region. As the thickness of the boundary layer approaches the radius of the pipe ($\delta \simeq D/2$) a fully developed velocity profile is established, which is the same for all liquid slugs, long enough for this to happen. The rate of advance of a Taylor bubble depends on the centerline velocity in the liquid of the preceding slug. If adjacent slugs are each long enough to have $\delta \simeq D/2$, then the centerline liquid velocities are the same, adjacent Taylor bubbles will advance at the same speed and no overtaking will take place. The result will be stable slug flow. However, in the entry region short high frequency slugs exist of variable length. These slugs are too short for the boundary layer thickness to be fully developed, as is shown in Fig. 1c. As a result, the centerline liquid velocities preceding successive Taylor bubbles are different. Since the rise velocity of the bubble nose depends on the liquid velocity at the rear part of the slug core, V_{t2}, which is sustained by the undeveloped slug is different from V_{t1}. When two such slugs merge as a result of overtaking, a single slug is created, whose length is approximately the sum of the two. This process continues (if the entry distance is long enough) until the length of all slugs is greater than that needed to create the fully developed profile associated with $\delta \simeq D/2$. If the minimum stable slug length is designated as l_s, then the slug lengths observed should be that resulting from the merger of two slugs one of which at least is shorter than l_s. Thus, slug lengths observed in the fully developed region should be practically greater than l_s.

When observed in a coordinate system moving with the translational velocity of the slug, V_t, the system resembles that of turbulent flow in a conduit with a sudden expansion. The hydrodynamics of such a sudden expansion in conduits has been discussed by Bradshaw [12]. In Fig. 2, the complicated nature of the flow is illustrated and its similarity to mixing in horizontal slug flow illustrated. It involves a relaxation of the turbulent boundary-layer into a recirculating flow region, formed between the separation point and the reattachment point, where a stream line anchors to the wall and a new wall boundary layer is formed. Downstream, the new boundary layer is redeveloped until some flow state can be identified where all

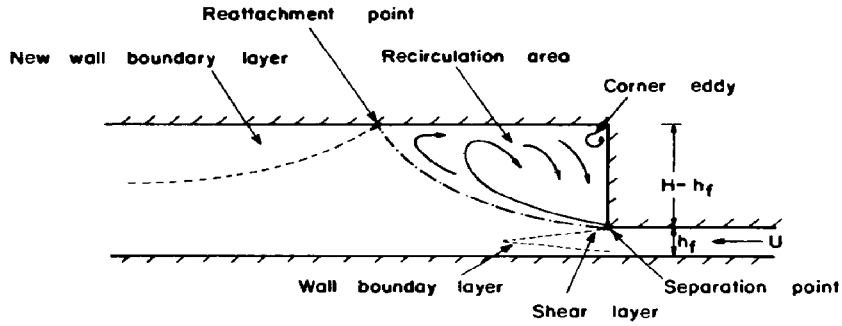

Fig. 2. Flow characterization due to a sudden expansion.

"memory" of the severe effects of separation and reattachment on the turbulence structure is gone. For a horizontal two-dimensional expansion, a distance as long as 25 times the layer thickness at the reattachment point is required before the "memory" of the effects of reattachment on the turbulent structure are gone [12]. In the recirculation zone, back flow velocities of one order of magnitude less than the mean velocity are observed and its length is about (6–7)H. This is equivalent to the length of the slug mixing zone, l_m [1]. Since a positive high pressure gradient (in moving coordinates) is associated with the slug front, the boundary layer on the lower wall is unstable, and thus the mixing process in the slug front may extend to the lower wall.

No attempt is made here to solve for the complicated phenomena associated with the mixing zone. However, based on the above facts, it is assumed here that the mixing process taking place at the slug front results in a uniform velocity distribution at the end of this region, where the wall boundary layer recovery is initiated.

The governing equations

Figure 1a shows the process of mixing and boundary layer redevelopment presented in a stationary coordinate system. At $x = 0$ the local velocity is uniform and equal to V_{LLS}. At increasing x the velocity distribution consists of $v = v(y)$, $y \leqslant \delta$ and $v = V_0$ for the outer region. The corresponding picture in a coordinate system moving upward with a velocity, V_t, is shown in Fig. 1b. The boundary layer velocity is $u(y)$ and the outer velocity is U_0.

In a moving coordinate system the integral forms of the momentum equations for the boundary-layer region and the external flow are respectively:

$$\frac{\mathrm{d}}{\mathrm{d}x}\int_0^{\delta} 2\pi(R-y)u^2\,\mathrm{d}y - U_0\frac{\mathrm{d}}{\mathrm{d}x}\int_0^{\delta} 2\pi(R-y)u\,\mathrm{d}y = \frac{2\pi R\tau_w}{\rho} - \frac{\pi[R^2-(R-\delta)^2]}{\rho}\frac{\mathrm{d}P}{\mathrm{d}x} \quad (1)$$

$$U_0\frac{\mathrm{d}}{\mathrm{d}x}\int_0^{\delta} 2\pi(R-y)u\,\mathrm{d}y + \frac{\mathrm{d}}{\mathrm{d}x}[(R-\delta)^2U_0^2] = -\frac{(R-\delta)^2}{\rho}\frac{\mathrm{d}P}{\mathrm{d}x} \quad (2)$$

where:

$$-\frac{\mathrm{d}P}{\mathrm{d}x} = \rho g_x - \frac{\mathrm{d}p}{\mathrm{d}x} \quad (3)$$

and:

$$\rho \simeq \rho_L(1-\alpha_{LS}).$$

α_{LS} is the gas holdup within the liquid slug and R is the tube radius. Note that the momentum of the gas bubbles within the liquid slug has been neglected since $\rho_G \ll \rho_L$. Equation (2) is the integral form of the Euler equation for the external flow region and can be reduced to its differential form:

$$U_0\frac{\mathrm{d}U_0}{\mathrm{d}x} = -\frac{1}{\rho}\frac{\mathrm{d}P}{\mathrm{d}x}. \quad (4)$$

Substituting the following non-dimensional variables:

$$\eta = r/R = \frac{R-y}{R};\quad X = x/D$$

$$\Delta = \delta/R;\quad \xi = \frac{u}{V_t}\quad \left(\text{and } \xi_0 = \frac{U_0}{V_t}\right) \quad (5)$$

eqs (1, 4) read, respectively:

$$\frac{\mathrm{d}}{\mathrm{d}X}\int_{1-\Delta}^{1}\xi^2\eta\,\mathrm{d}\eta - \xi_0\frac{\mathrm{d}}{\mathrm{d}X}\int_{1-\Delta}^{1}\xi\eta\,\mathrm{d}\eta = \frac{2\tau_w}{V_t^2} - \frac{(2-\Delta)\Delta}{2\rho V_t^2}\frac{\mathrm{d}P}{\mathrm{d}X} \quad (6)$$

$$\xi_0\frac{\mathrm{d}\xi_0}{\mathrm{d}X} = -\frac{1}{\rho V_t^2}\frac{\mathrm{d}P}{\mathrm{d}X}. \quad (7)$$

Note that the pressure term can be eliminated by combining eqs (6, 7).

An overall volumetric balance for the gas and liquid phases between the conduit entry and any cross-section through the liquid slug is now performed, whereby:

$$V_S = \left(\frac{W_L}{\rho_L}+\frac{W_G}{\rho_G}\right)\Big/A = V_{LS}+V_{GS} = V_{LLS}(1-\alpha_{LS}) + V_{GLS}\alpha_{LS} \quad (8)$$

and:

$$V_{GLS} = V_{LLS} + v_{G0} \quad (9)$$

where A is the total cross-sectional area of the conduit, V_{LS}, V_{GS} are the superficial velocities, and V_{LLS}, V_{GLS} are the actual average velocities within the liquid slug of the liquid and gas respectively. v_{G0} is the rise velocity of the entrained gas bubbles within the liquid slug. For zero rise velocity, $v_{G0} = 0$ and $V_{LLS} = V_{GLS}$, eq. (8),

reads:

$$V_S = V_{LS} + V_{GS} = V_{LLS} = V_{GLS} \tag{10}$$

while for non-zero slip velocity eqs (8, 9) yield:

$$V_{LLS} = V_S - \alpha_{LS} v_{G0}. \tag{11}$$

In a stationary coordinate system, the average liquid velocity V_{LLS} in eq. (8) is related to the local velocity distribution by:

$$V_{LLS} = \frac{\int_0^\delta 2\pi(R-y)(V_t-u)\mathrm{d}y + (R-\delta)^2(V_t-U_0)}{\pi R^2} \tag{12}$$

or in its non-dimensional form:

$$V_{LLS}/V_t = 2\int_{1-\Delta}^{1}(1-\xi)\eta\,\mathrm{d}\eta + (1-\xi_0)(1-\Delta)^2. \tag{13}$$

Equation (12) or (13) with eq. (8) represent the kinematic condition to be fulfilled by the local velocity profile. A power law model for the velocity profile of the liquid is now utilized assuming that the form of the equation remains unchanged in the presence of bubbles in the slug.

$$\frac{v}{V_0} = \frac{V_t-u}{V_t-U_0} = \left(\frac{y}{\delta}\right)^{1/n} \quad \text{for } 0 < y < \delta \tag{14}$$

or:

$$\frac{u}{V_t} \equiv \xi = 1-(1-\xi_0)\left(\frac{1-\eta}{\Delta}\right)^{1/n}. \tag{15}$$

Substituting eq. (15) into eq. (13) and integrating yields a relationship between the local boundary-layer thickness and the local external velocity (of the invicid core):

$$\xi_0 = 1 - \frac{V_{LLS}}{V_t}\Big/\left\{\frac{2n}{(2n+1)(n+1)} \times \Delta[n(2-\Delta)+(1-\Delta)]+(1-\Delta)^2\right\}. \tag{16}$$

In vertical upward slug flow, due to buoyancy forces, $v_{G0} \neq 0$ and the velocity of the gas in the Taylor bubble, V_{GT}, is given by [13–15]:

$$V_{GT} = C_1 V_{LLS} + 0.35\sqrt{(gD)} \tag{17}$$

where C_1 is a proportionality constant related to the velocity profile within the liquid slug. Nicklin *et al.* [13] suggested a value of 1.2 for C_1 while Nicolistas *et al.* [14] reported a value of 1.24, both out of experimental data.

A mass balance in moving coordinates on the gas phase reads:

$$(V_t - V_{GT})\alpha_{TB} = (V_t - V_{GLS})\alpha_{LS} \tag{18}$$

where α_{LS}, α_{TB} are the gas holdup in the liquid slug and in the Taylor-bubble regions, respectively.

Substitution of eqs (9, 17) into eq. (18) yields:

$$V_t = \frac{V_{LLS}\left(C_1 - \frac{\alpha_{LS}}{\alpha_{TB}}\right) + 0.35\sqrt{(gD)} - v_{G0}\frac{\alpha_{LS}}{\alpha_{TB}}}{\left(1-\frac{\alpha_{LS}}{\alpha_{TB}}\right)}. \tag{19}$$

For the case of pure liquid slug, $\alpha_{LS} = 0$, eqs (8, 19) reduce to:

$$V_{LLS} = V_S; \quad \alpha_{LS} = 0 \tag{8a}$$

$$V_t = C_1 V_S + 0.35\sqrt{(gD)}. \tag{19a}$$

The constant C_1 is determined by eq. (16). For example, for $\alpha_{LS} = 0$, $U_0 \to 0.35\sqrt{(gD)}$ ($\xi_0 \to [0.35\sqrt{(gD)}/V_t]$) as $\Delta \to 1$, and eq. (16) yields:

$$\frac{V_t}{V_{LLS}} = \frac{V_t}{V_S} = \frac{(2n+1)(n+1)}{2n^2} + \frac{0.35\sqrt{(gD)}}{V_S} \overset{n=7}{\to} 1.225 + \frac{0.35\sqrt{(gD)}}{V_S}. \tag{20}$$

(Vertical slug, $\alpha_{LS} = 0$.)

Thus, C_1 in eqs (17, 19) equals 1.225. The constant 1.225 is an outcome of the 7th power law for turbulent flow and it is in agreement with previous empirical results and other analytical treatments [1, 2, 6, 13–15].

Utilizing the velocity profile, eq. (15) and the kinematic condition, eq. (16) in the momentum balance, eq. (6) yields:

$$\left\{(1-\Delta)+\frac{n}{(n+2)}(1-\xi_0)\left(1-2\Delta+\frac{n}{(n+1)}\Delta\right) - \frac{n}{(n+1)}(2-\xi_0)\left[1-2\Delta+\frac{2n\Delta}{(2n+1)}\right]\right\} \times (1-\xi_0)\frac{\mathrm{d}\Delta}{\mathrm{d}X} + \left\{\frac{n}{(n+1)}\Delta(2-\xi_0)\left(1-\Delta+\frac{n}{(2n+1)}\Delta\right) - \frac{2n}{n+2}(1-\xi_0)\left(1-\Delta+\frac{n}{2(n+1)}\Delta\right)\right\}\Delta\frac{\mathrm{d}\xi_0}{\mathrm{d}X} = \frac{2\tau_w}{\rho V_t^2} - \frac{\Delta(2-\Delta)}{2\rho V_t^2}\frac{\mathrm{d}P}{\mathrm{d}X} \tag{21}$$

where the pressure term is determined by eq. (7), and ξ_0, $\mathrm{d}\xi_0/\mathrm{d}X$ are obtained from eq. (16). The wall shear stress, τ_w, is obtained locally (based on the 7th power law) by:

$$\frac{\tau_w}{\rho} = 0.0225 V_0^2\left(\frac{\nu_L}{\delta V_0}\right)^{1/4}. \tag{22}$$

Integration of eq. (21) with the initial condition $\delta = \delta_0$ at $x = 0$ ($\Delta = \Delta_0$ at $X = 0$) yields the local boundary-layer thickness, local velocity profile (with local V_0 or U_0) and local pressure gradient as functions of position, x. The resulting $\mathrm{d}P/\mathrm{d}X$ is positive (the pressure rises along the slug) and as $\delta \to D/2$ ($\Delta \to 1$) the pressure gradient is expected to approach the pressure gradient for the fully developed velocity distribution. However, as $\Delta \to 1$ the resulting $\mathrm{d}P/\mathrm{d}x$ in the above (approximate) formulation does not match with the expected equilibrium pressure gradient. Therefore, it seems that the exact evaluation of the pressure gradient by eq. (7) is questionable. The elimination of the local pressure gradient at the entry region in pipes by a similar simplified treatment for the entry of a pipe was criticized with the identical connotation [16]. To avoid this problem, the calcu-

lated pressure drop in the fully developed region may be utilized. This pressure gradient is determined by setting the RHS of eq. (21) to zero with $\Delta \to 1$ and $V_0 \to 1.225 V_{LLS}$. Combining with eq. (22), this yields:

$$\frac{1}{\rho V_t^2}\left(\frac{dP}{dx}\right)_{dev.} = \frac{4\tau_w}{\rho V_t^2} = 0.09\left(\frac{2\nu_L}{D V_t}\right)^{1/4}\left[1.225\frac{V_{LLS}}{V_t}\right]^{7/4}. \quad (23)$$

Application to horizontal slug flow

Due to buoyancy forces in horizontal pipes the Taylor bubbles and the small entrained gas bubbles within the liquid slug tend to agglomerate on the upper tube wall, with zero slip velocity in the flow direction ($v_{GO} = 0$, $V_{GLS} = V_{LLS} = V_S$). This results in an asymmetric gas (and liquid) holdup distribution with an asymmetric redevelopment of the wall boundary layers [4]. However, such an idealized axisymmetric redevelopment of the boundary layers in horizontal slug flow may be assumed if the mixing processes taking place at the slug front results in a complete separation of the lower wall boundary layer and turbulent mixing and breakage forces within the slug are high enough to prevent agglomeration of the entrained gas bubbles on the upper tube wall. In this case, a uniform velocity profile is obtained at the end of the mixing region. Thus, at the point where a new boundary layer is initiated the velocity distribution of the inviscid core is uniform, $V_0 = V_{LLS} = V_S$. Under these conditions, the mathematical formulation is identical with the axisymmetric vertical upward slug flow (with $g_x = 0$ in eq. (3)). As no buoyancy forces exist in the flow direction, $\xi_0 \to 0$ as $\Delta \to 1$. For this case eq. (16) yields:

$$\frac{V_t}{V_S} = \frac{(2n+1)(n+1)}{2n^2}^{n=7} \to 1.225. \quad (24)$$

RESULTS AND DISCUSSION

The minimum stable slug length l_s, is the length over which complete recovery of the wall boundary layers takes place, thereby $\delta \to D/2$ or $\Delta \to 1$. As it has been noted earlier, integration of eq. (21) can be carried out once dP/dX is prescribed. The results presented here correspond to a fully-developed pressure gradient as is given in eq. (23). The predicted minimum stable slug lengths based on dP/dx as obtained by the Euler equation outside the boundary-layer are 30–40% lower due to the lower pressure gradients obtained by eq. (7).

The lower set of curves in Fig. 3 shows the variation of the dimensionless minimum stable slug length, l_s/D, with Reynolds number, DV_s/ν, as calculated from the theory. The data of Fernandes [17] for the mean slug length is shown as the circles. These measurements were made in a vertical Plexiglass tube, 0.0507 m in diameter and 11.1 m long, using air–water. The data covered the full range of flow rate space for which the slug flow pattern was observed. For these data α_{LS} varied from about 0.24 to 0.29 and α_{TB} around ≈ 0.86. For reference, the limiting curve for $\alpha_{LS} = 0$ is also presented. The results are insensitive to the value of α_{TB} in the range 0.80–0.90 with the change in l_s/D being less than 3%.

As is shown in Fig. 3, all experimental average slug lengths are higher than the minimum stable slug length predicted by the theory. The wide scatter (RMS of 40% for horizontal [6], and 20% in vertical flows [17]) usually obtained in experimental studies of the stable slug length, is expected in view of the random nature of overlapping involved in the stabilization process. As a matter of fact, any combination of two slugs, one of which (at least) being shorter than the minimum stable length, may be involved in the overlapping process taking place at the entry region. Thus, the most probable slug length may differ from the minimum

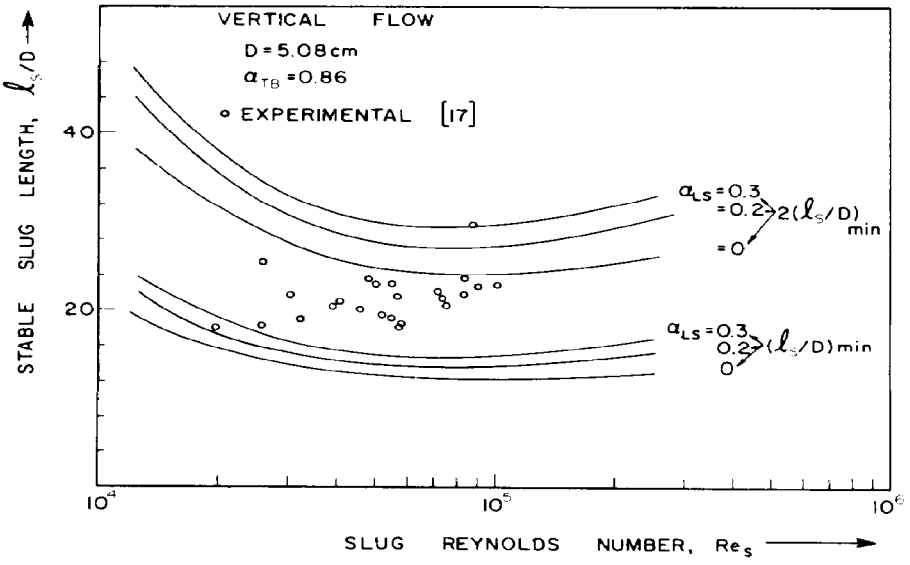

Fig. 3. Stable slug length in vertical flow: comparison with experiments.

stable slug length, probably being two times the minimum length (resulting from the merger of two slugs each slightly shorter than l_s). Indeed, all average experimental values are confined between the minimum slug length and twice of that length. Note, that the comparison in Fig. 3 does not take into account the length of the mixing region at the front of the slug. However, guided by the studies of Bradshaw discussed above [11, 12] and the results of Dukler and Hubbard [1] this distance is of the order of $l_m/D \simeq 3$–5 and is within the uncertainty range due to the random nature of the overlapping process in the developing region. Thus, the mixing length, which is of importance for slug transport modelling, may not be critical in estimating the range of the total slug length, which includes both the recovery distance of the wall boundary layer and the mixing length.

The variation of the minimum stable slug length with Re_s in horizontal flow is presented in Fig. 4, and compared with Hubbard's [6] experimental data obtained in 0.038 m i.d. pipe for air–water horizontal flow. Again the observed average slug lengths are essentially bounded by the minimum stable slug length curve and twice that value.

Figure 5 represents the ratio of the translational velocity of the Taylor bubble to the average liquid velocity in the liquid slug, as obtained by eq. (19). As it has been shown, this ratio, V_t/V_{LLS} is constant for horizontal slug flow and for a 1/7th power velocity distribution it becomes 1.225 (eq. 24). For vertical slug flow, this ratio is always larger due to the rise velocity of the Taylor bubble relative to the liquid slug. For high slug Reynolds V_t/V_{LLS} approaches a constant value, which reduces to 1.225 for $\alpha_{LS} = 0$.

The constancy of V_t/V_{LLS} for the horizontal slug flow results in a monotonically increasing l_s/D with Reynolds number as shown in Fig. 4. On the other hand the decrease in V_t/V_{LLS} with Re for upward slug flow creates the minima observed in Fig. 3.

CONCLUSIONS AND FINAL REMARKS

The proposed model represents an attempt to explain the physical mechanisms associated with slug length stabilization. The concepts of recurrent relax-

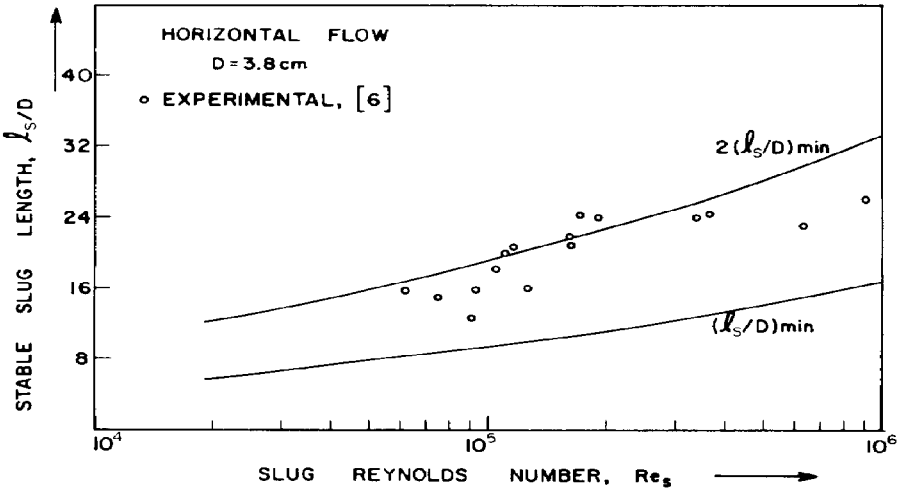

Fig. 4. Stable slug length in horizontal flow: comparison with experiments.

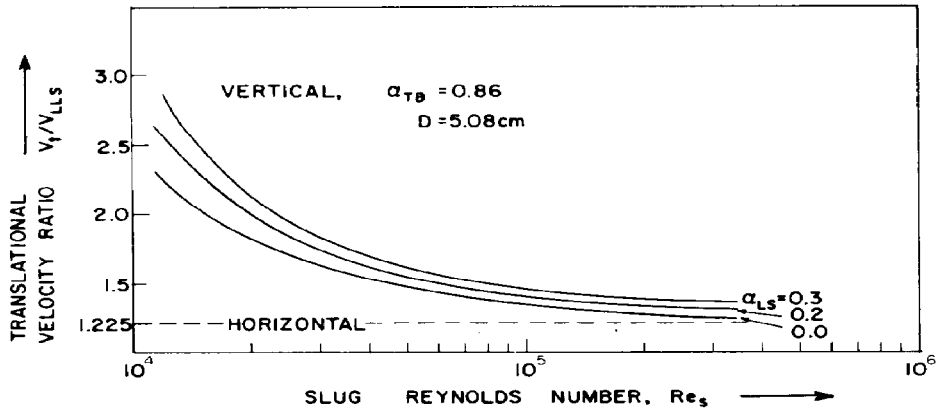

Fig. 5. Slug translational velocity ratio.

ation and development of the wall boundary layers has been found useful in predicting stable slug lengths. This provides a method to effect closure for previously existing models for this flow pattern.

The minimum stable slug length is that length required for re-establishment of a fully developed velocity profile at the rear of the liquid slug. The stable slug length should be that resulting from the merger of two slugs, one, at least, being shorter than the minimum stable slug length. A variety of observed slug lengths, at the fully developed region, is to be expected in view of the random nature of the re-establishment of turbulent boundary layers and the overlapping processes along the entry region.

The specific geometry of the test installation, i.e. the liquid and gas feeding devices, probably affects the distance required for the stabilization process—the entry region length, and the distribution of the observed slug lengths. However, far away downstream, at the fully developed region, the probable average slug length is reasonably predicted for a wide range of slug Reynolds numbers in horizontal and vertical configurations.

It is finally to be noted that hydrodynamic mechanisms of a recurrent distortion and recovery of the wall boundary layers may be of importance in modelling transport rates in slug flows.

NOTATION

C_1	constant defined in eq. (17)
D	tube diameter, m
g	gravity acceleration, m/s^2
l_s	liquid slug length, m
n	the power in the general power law velocity profile
p	local pressure in the liquid slug, N/m^2
P	pressure term defined in eq. (3), N/m^2
r	radial distance, m
R	tube radius, m
Re_s	slug Reynolds number
u	local velocity in x direction viewed in translating coordinate, m/s
U_0	velocity of the inviscid core viewed in translating coordinates, m/s
v	local velocity in the flow direction, m/s
v_{GO}	slip velocity of entrained gas bubbles, m/s
V_{GT}	Tailor bubble rise velocity, m/s
V_{LS}, V_{GS}	liquid and gas superficial velocities, m/s
V_{LLS}, V_{GLS}	actual average velocity of the liquid and gas within the liquid slug, m/s
V_S	sum of liquid and gas superficial velocities, m/s
V_t	slug translational velocity, m/s
x	flow direction, measured in translating coordinate system, m
X	dimensionless distance in the flow direction
y	coordinate perpendicular to the flow direction, m

Greek letters

α_{LS}	average gas holdup within the slug
α_{TB}	average gas holdup in the Taylor bubble region
δ	boundary layer thickness, m
δ_0	initial boundary layer thickness, m
Δ	nondimensional boundary layer thickness
ξ	nondimensional velocity within the recovering boundary layer
ξ_0	nondimensional velocity of the invicide core
η	nondimensional perpendicular distance
μ_L	liquid viscosity, N s/m^2
ν_L	liquid kinematic viscosity, m^2/s
ρ_L, ρ_G	liquid and gas densities, kg/m^3
ρ	mixture density, kg/m^3
τ_w	wall shear stress in the slug back region, N/m^2

REFERENCES

[1] Dukler A. E. and Hubbard M. G., *Ind. Engng Chem. Fundam.* 1975 **14** 4.
[2] Nicholson M. K., Aziz K. and Gregory G. A., *Can. J. Chem. Engng* 1978 **56** 653–663.
[3] Taitel Y. and Dukler A. E., *Int. J. Multiphase Flow* 1976 **3** 47–55.
[4] Moalem Maron D., Yacoub N. and Brauner N., *Heat Mass Transfer* 1982 **9** 333–342.
[5] Fernandes R., Semiat R. and Dukler A. E., *A.I.Ch.E. J.* 1983 **29** 981.
[6] Hubbard M. G., Thesis, University of Houston 1965.
[7] Moissis R. and Griffith P., *J. Heat Transfer* 1962 **84** 29.
[8] Moissis R., *J. Heat Transfer* 1963 **85** 366.
[9] Taitel Y., Barnea D. and Dukler A. E., *A.I.Ch.E. J.* 1980 **26** 345–354.
[10] Barnea D. and Brauner N., *Int. J. Multiphase Flow* 1985 **11**(1).
[11] Brauner N. and Moalem Maron D., *Chem. Engng Sci.* 1983 **38** 775.
[12] Bradshaw P., *Topics in Applied Physics, Turbulence* 12(3) Chapter 3, Springer, Berlin 1976.
[13] Nicklin D. J., Wilkes J. O. and Davidson J. F., *Trans. Inst. Chem. Engrs* 1974 **40** 61.
[14] Nicolistas A. J. and Murgatroyd W., *Chem. Engng Sci.* 1968 **23** 934.
[15] Collins F. F. de Moraes, Davidson J. F. and Harrison D., *J. Fluid Mech.* 1978 **89** 497.
[16] Dealy J. M., *A.I.Ch.E. J.* 1966 **11**(4) 745.
[17] Fernandes R. C. Ph.D. Thesis, University of Houston 1981.